

# Calibrating Astronomical Exposures Contaminated by Out-of-Focus (Pupil) Camera Reflections

F. Valdes<sup>1</sup>

**National Optical Astronomy Observatories  
Science Data Management**

Draft: November 8, 2013

---

<sup>1</sup>NOAO Science Data Management, P.O. Box 26732, Tucson, AZ 85732

## Table of Contents

<b>Introduction</b>	<b>1</b>
<b>1 The Calibration Model</b>	<b>1</b>
<b>2 Calibration Algorithms</b>	<b>3</b>
2.1 Dark Energy Camera . . . . .	3
2.2 Mosaic Imager . . . . .	5
2.3 One Degree Imager . . . . .	6

## List of Figures

1	NOAO DECam - Dark sky stacks in u (left) and z (right). The g filter also has a comparable pattern but not other filters. The data was calibrated just with dome flat fields which were not gain corrected. In addition to illustrating the size and amplitude of the pattern it also demonstrates that the amplitude in dome flats is not such as to "flat field" the pattern away. The bright spot at the center of the u filter is a different effect which is still not well understood. . . . .	4
2	NOAO MOSAIC - On the left is a raw exposure (Bw filter). A dome would be similar without the sources. In the middle is the calibrated version after a pattern corrected dome flat was applied and the background pattern removed. On the left is the pattern extracted from a dark sky stack of a number of exposures. . . . .	5
3	WIYN ODI - The pupil pattern seen in the 4 central OTAs of ODI. This was extracted using the ratio of g-band exposures between the stronger layer and the weaker, more diffuse layer. There are two bad cells visible. . . . .	7

## Introduction

A problem that occurs in many astronomical cameras is a double reflection that superposes a weak, highly defocused pattern on an exposure. The double reflection occurs between various optical elements (e.g. filter(s), the dewar window, corrector(s)) or the detector surface itself. It is generally weak (1%-10%) because, naturally, every effort is made to avoid reflections through coatings, alignments, etc. This pattern is commonly referred to as a pupil pattern or pupil ghost. Removing this pattern in the presence of detector pixel response variations of comparable magnitude in complex, mosaic detector arrays is one of the most challenging calibration problems for such cameras. Compounding the challenge is a confusion over the calibration model. This paper provides a mathematical description of the calibration model and then provides some examples of reflection patterns in several cameras and some algorithms used or investigated for removing the pattern.

## 1 The Calibration Model

The imaging model is represented as

$$O_i^j = (I_i + I_b(1 + \alpha p_i) + \beta f_i)r_i^j \quad (1)$$

where  $O_i^j$  are observed (raw) counts at position  $i$  in detector  $j$ ,  $I_i$  and  $I_b$  are the source signal,  $p_i$  is the reflection pattern with an amplitude  $\alpha$  relative to  $I_b$ ,  $f_i$  is a fringe pattern with an amplitude  $\beta$  and  $r_i^j$  are the pixel responses. The separation of the source signal into variable,  $I_i$ , and fixed,  $I_b$  components is a representational choice that is useful to interpret the calibration model derived in this section. Implicit in this model is that terms are bandpass dependent and pixel area variations are merged into responses. Typically  $\beta$  is zero except in a few redder filters.

In this model the source and patterns are considered independent of the detector and are decomposed into a spatial pattern with an exposure dependent amplitude. The amplitudes are further represented as something that scales with some measure of the light,  $I_b$ , though there is no requirement that  $\alpha$  be interpreted as a fixed reflection coefficient nor that  $\beta$  actually depend on the broad-band light. Typically the fringe pattern amplitude depends on the strength of the narrow night sky lines in the bandpass but making it relative to  $I_b$  does affect the generality. We make the assumption that the shapes of the patterns don't change with exposure since they are caused by a very out of focus image of the field for the reflection pattern and the diffuse night sky lines.

For clarity in the next part of the derivation we drop the  $i$  and  $j$  indices. Next we write the imaging model for an on-sky exposure  $S$  to be calibrated with a flat field exposure  $F$ . Note that here we assume the data have been already corrected for instrumental biases (i.e. electronic and dark biases). A flat field is generally a master calibration created from a number of individual dome flat field exposures.

$$S = (I_s + I_b(1 + \alpha p + \beta f))r_s \quad (2)$$

$$F = (1 + p)r_f \quad (3)$$

Note that the pixel responses are not assumed to be the same due to differences in the source spectrum and, possibly, illumination of the telescope. For the flat field we assume the true source is uniform ( $I + I_b = I_f = \text{constant}$ ), which is the definition of a flat field, and we can assume a global normalization to avoid carrying this constant around. Also the dome flat is assumed not to produce fringing in the detector. If one wants to normalize each detector in a mosaic camera separately, the relative normalization values can be folded into the  $r_f$  which then are reflected in the illumination function as defined below.

We also define  $\alpha p$  as being just  $p$  in the flat field. Then the  $\alpha I_b p$  factor is the relative scaling from the flat field to the sky exposure. We define the following quantities which appear later.

$$R \equiv r_s/r_f \quad (4)$$

$$L \equiv R/(1+p) \quad (5)$$

$$F' \equiv FL \quad (6)$$

$$F'' \equiv F - pr_f \quad (7)$$

The first,  $R$ , represents the difference in pixel responses between the dome flat field and the sky exposure. This quantity is often called the "illumination" pattern and is typically derived as a smooth spatial function over an amplifier but with discrete jumps between amplifiers and detector arrays. The quantity  $L$  will become apparent below as the gain correction due to the reflection pattern, the  $(1+p)$  term, and the illumination response, the  $R$  term. The last quantities,  $F'$  and  $F''$ , are two ways of modifying the dome flat field to account for the reflection pattern.

Rearranging terms produces the following calibration model.

$$\frac{S}{F'} = \frac{S}{F''} = I_s + I_b + \alpha I_b p + \beta I_b f \quad (8)$$

This result demonstrates several things. First is that we get the true sky signal,  $I_s + I_b$  plus the additive reflection patterns by correcting the observed dome flat field. Second the debate over whether one subtracts the reflected light pattern from the flat field or "flat fields" the flat is resolved by both yielding equivalent results. So the choice is then about which correction is easier to determine. At this point the pattern scaling term  $I_b$  can be interpreted as the (mean) sky background. If the cumulative light of sources and/or light from outside of the field of view contributes to the strength of the reflection pattern this is accounted for by the exposure dependent amplitude term  $\alpha_s$ .

Now consider what happens if the dome flat is used without a correction. Writing that operation produces

$$\frac{S}{F} = LI_s + RI_b \frac{1 + \alpha p}{1 + p} + RI_b \frac{\beta f}{1 + p} \quad (9)$$

First we see that the sky signal has a spatially varying gain calibration error given by  $L$ . Second, if  $\alpha$  is nearly one the reflection pattern disappears in the flat fielded data. Thus one might be led to *incorrectly* believe, by visual inspection, that the data have been well flat fielded. This near equality has been seen in some (but not all) instruments which is why we demonstrate this result. Finally,

in (9) we can easily see that in the absence of a reflection pattern, where  $p = 0$  and  $L = R$ , the standard calibration model of applying a dome flat field, an illumination correction, and subtracting a fringe pattern is obtained.

The calibration model that we recommend is that using  $F'$  where the dome flat field is corrected by "flat fielding" with a normalized pattern. This is shown explicitly below.

$$I_s + I_b = \frac{S - \alpha S_b p}{FL} - \beta I_b f = \frac{S}{FL} - \alpha I_b p - \beta I_b f \quad (10)$$

where  $I_b \equiv S_b/(FL)$ . The two forms on the right differ by whether one subtracts the reflection pattern in the raw or in the flat fielded data. One could also just leave the pattern in the flat fielded data as part of the background. However, if the pattern is sufficiently strong, leaving it can cause other processing problems such as in stacking exposures.

There are three independent quantities in the calibration model relating to the reflection pattern;  $R$ ,  $p$ , and  $\alpha$ . For gain calibration only the combination of two, namely  $L = R/(1 + p)$ , is needed. For fringe subtraction the quantities  $\beta$  and  $f$  are, obviously, also needed.

## 2 Calibration Algorithms

Teasing out the various quantities for the calibration model is an approximation process because of trade-offs between coupled terms that are often impossible to cleanly separate. This sometimes involves special types of exposures and sometimes iterative removal starting with the strongest terms first. In the examples below the difference in approaches are the result of the differences in strength of the reflection (i.e.  $\alpha$ ), the variation in the detector responses, and the size and diffuseness of the pupil pattern.

### 2.1 Dark Energy Camera

The Dark Energy Camera (DECam) at the Cerro Tololo Inter-American Observatory (CTIO) Blanco telescope has a large pattern in some filters (see figure 1). This has the challenges that it spans many CCDs and, with the detector response variations, is difficult to identify in dome flat fields. While the pattern is not clearly visible in dome flat fields it can easily be seen in dark sky flat field stacks, even with just dome flat calibrated exposures, which tells us that  $\alpha$  is not near one in the calibration model. It can also be seen in photometric "star flats" as discussed below.

The use of star flats attacks the problem directly through the calibration model. Since it is based on local background subtracted photometry, symbolized by  $S_i^* \equiv \text{phot}[S_i/F_i]$  for a source at position  $i$ , the background term in (10) is eliminated. Now consider taking many dithered exposures of a fairly dense field in photometric conditions. Identify all instances of the same star by the label  $j$  so that  $S_{ij}^*$  is the photometric flux of star  $j$  at position  $i$ . With enough stars per exposure and large enough dithers so that  $i$  for a particular star samples significantly different parts of the field the function  $L$  can be determined by

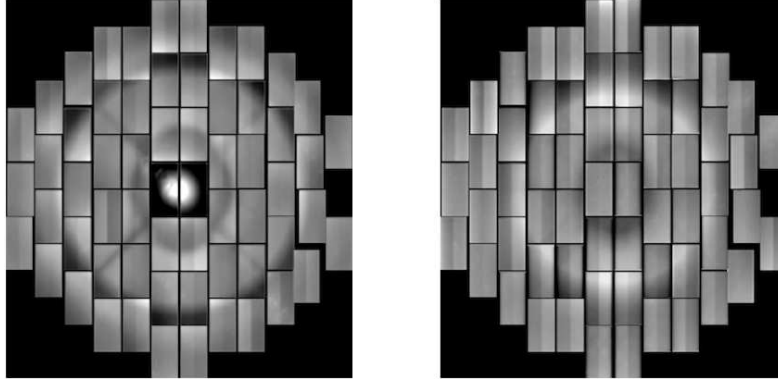


Figure 1: NOAO DECam - Dark sky stacks in u (left) and z (right). The g filter also has a comparable pattern but not other filters. The data was calibrated just with dome flat fields which were not gain corrected. In addition to illustrating the size and amplitude of the pattern it also demonstrates that the amplitude in dome flats is not such as to "flat field" the pattern away. The bright spot at the center of the u filter is a different effect which is still not well understood.

$$\min_{ij} \left[ \left( A_i S_{ij}^* - \overline{A_i S_{ij}^*} \right)^2 \right] \quad (11)$$

where  $\min$  means to minimize over all photometric values and the mean is over all instances of star  $j$  and  $A \equiv 1/L$  (defined for convenience). The separation of  $A$  from the aperture photometry assumes that it is effectively constant over the aperture. Note that even if conditions are not perfectly photometric, one can adjust by the relative zero points derived from all common stars or matches to magnitudes in a reference catalog. Equation (11) is in terms of linear fluxes but it could also be cast and solved in terms of instrumental magnitudes if desired.

There are currently two methods being used for solving (11). One is based on dividing up  $A_i$  into cells (also called "super pixels") and not using any assumption other than a constant value per cell. The cell sizes are 512 x 512 (which is coincidentally the about the same as ODI OTA cells discussed elsewhere). The other method is a functional approach. The cell method is currently in use with the NOAO Community Pipeline.

A point to note is that even in the absence of a reflection, the star flat method still produces a gain calibration function which is purely due to the illumination correction  $R$ . In the presence of a reflection some assumptions on the shape of the pattern, i.e., a smooth donut-shaped pupil pattern, would be needed to separate illumination contributions from the reflection component. However, for the purposes of the photometric gain calibration the function  $A$  is sufficient in and of itself.

Since the derivation of the gain calibration  $A$  depends on specific observational data, it is used in the NOAO Community Pipeline as a static external calibration. The pipeline does not apply the pupil subtraction since, as just noted, it is not possible to cleanly separate the reflection pattern from the illumination corrections with just the star flat derived  $A$  function nor select the amplitude factor  $\alpha$ .

### Relation to the DES Calibration Model

The DES calibration model is nearly identical except for defining

$$p_{des} = p_{rf} \quad (12)$$

$$\alpha = 1 \quad (13)$$

and not explicitly using separate response terms for the dome flat field and the sky. However, the illumination function  $R$  is implicit in the star flat gain calibration.

## 2.2 Mosaic Imager

The NOAO Mosaic Imager (MOSAIC) at the Kitt Peak National Observatory (KPNO) Mayall telescope has a pronounced pupil pattern in a number of filters. Figure 2 shows an example of the pattern in a raw exposure and after it has been removed as described in this section. The pattern covers 4 CCDs and 4 or 8 amplifier images depending on readout mode. The pattern is sufficiently strong and stable that the center and edges of the pattern can be well determined and used in the calibration algorithms. It is also useful that the pattern does not cover all of any CCD.

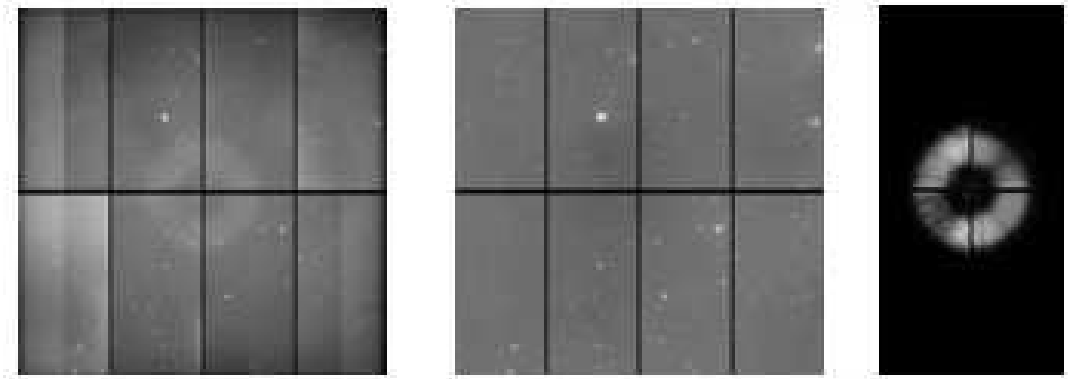


Figure 2: NOAO MOSAIC - On the left is a raw exposure (Bw filter). A dome would be similar without the sources. In the middle is the calibrated version after a pattern corrected dome flat was applied and the background pattern removed. On the left is the pattern extracted from a dark sky stack of a number of exposures.

The calibration model (10) is rewritten as

$$F_c \equiv F/(1 + p) \quad (14)$$

$$I = \frac{(S/F_c - \alpha p' - \beta f)}{R} \quad (15)$$

This shows the calibration as broken up into the steps of 1) correct the dome flat field, 2) apply the corrected flat field to the sky observation, 3) subtract a reflection pattern background, 4) subtract a fringe pattern, and 5) apply an illumination correction. Note that for the CCDs which are not affected by the pattern only the fourth step is needed and so the other steps are restricted to just the affected CCDs.

The first step is to find  $1 + p$  from the dome flat field. As seen in fig. 2 there are plenty of pixels not affected by the pattern, so we normalize each CCD by its mean over the unaffected areas. For dual-amp data the normalization is done by amplifier. This largely normalizes the dome response leaving a good view of the pattern. The pattern is then fit over all the affected CCDs simultaneously with radial and azimuthal functions. The knowledge of the inner and out edges of the pattern allows fitting an azimuthal background. The result is a model pattern  $p$ . Finally the pattern is removed from the dome flat field by adding 1, removing the normalizations, and dividing into the dome flat field. Note that because we fit a smooth function across the full ring in the four normalized CCDs, the flat field responses  $r_f$  are washed away.

For removing the background pattern from the on-sky exposures, a dark sky stack is created from a set of observations over one or more nights. The stack makes use of object detection masks as well as statistical clipping and various heuristics to remove exposures with large or very crowded sources and bad sky conditions (transparency and twilight contamination). The pattern,  $p'$ , is "scaped" off the stack using knowledge of the position and edges of the pattern to fit an azimuthal background function. The pattern amplitudes,  $\alpha$ , are determined for each exposure. Again it is very important to use object detection masks to deal with sources that fall in the pattern. Also weights based on the pattern are used. Finally, the scaled pattern,  $\alpha p'$ , is subtracted from the exposure. A note here is that the reflection pattern is derived in two different ways at two different times. This means the pattern is not required to be exactly the same in both the dome flat field and the sky exposures, hence denoting the pattern as  $p'$ .

If a pattern  $p'$  for the particular set of nights is obtained it is archived. If the set of exposures is not suitable for deriving the pattern then an earlier archived pattern is used.

The flat field correction described in the first step works perfectly in all cases. The background subtraction from the science exposures, however, can be problematic for some data because of the sources in the pattern. The automatic scaling algorithm works most of the time but there are cases that the eye can see as over or under subtracted. An individual could improve things with a more tedious trial-and-error subtraction and display.

If there is fringing in the particular filter the fringe pattern,  $f$ , is found by making a dark sky stack and subtracting a low-pass filtered version of the stack. The amplitude,  $\beta$ , is determined for each exposure with object masking and weighting to the regions where the fringe pattern amplitude is stronger.

After subtraction of the reflection and fringe pattern from all exposures, each with different scales  $\alpha$  and  $\beta$ , is completed then the illumination correction  $R$  is derived in a subsequent creation of a dark sky stack. Again we make use of object masking and statistical rejection to remove the effects of sources. As with deriving the reflection pattern, it is not always possible to obtain an illumination correction for a dataset. In this case an earlier archived illumination correction is used. The middle panel of figure 2 is after all the steps.



### 2.3 One Degree Imager

The One Degree Imager (ODI) at the Wisconsin-Yale-Indiana-NOAO (WIYN) Observatory 3.5m telescope has weak to modest strength patterns (see figure 3). These present some unusual challenges. The camera has three "layers" of filters (with only one used at a time) which, because of the differing distances, produce pupil patterns of differing sizes and diffuseness. The filters are currently not exactly repositioned into the beam which introduces a small amount of shift in the pattern relative to the focal plane. The camera is mounted on an alt-az telescope so the source field rotates. Finally, the detectors are orthogonal transfer arrays (OTAs) where each OTA is electronically divided into 64 cells; i.e. there are 64 amplifiers per OTA and multiple OTAs in a mosaic.

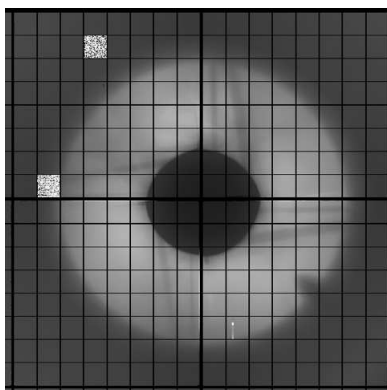


Figure 3: WIYN ODI - The pupil pattern seen in the 4 central OTAs of ODI. This was extracted using the ratio of g-band exposures between the stronger layer and the weaker, more diffuse layer. There are two bad cells visible.

Because of the large number of small cells the challenge with separating the response term,  $R$ , and even seeing the pattern in dome flats, is large.

The algorithms to address the reflection in ODI are still evolving. The approaches currently are based on obtaining a pattern template for which the amplitude factors,  $\alpha_f$  and  $\alpha_s$ , are then determined. This is the same algorithm as used successfully with the NOAO MOSAIC camera.

The challenge is in isolating the pattern. Several interesting approaches have been explored for "flat fielding" the cell gains independent of the pattern. One method is to use dome flats taken in a filter layer that has a fainter pattern as a reference flat field for dome flats in the layer with the stronger pattern. This has been tried both with the same filter and with different filters in the reference layer. For one combination of the same filter in different layers this works fairly well (figure 3).

Another very promising approach is to use a very broad band filter (actually just clear glass) to produce the reflection and then flat field it with an exposure that has no filter in the optical path. The problem with this is getting a (cheap) clear glass insert that doesn't smear out the structure relative to that in the optical quality filters.

A star flat approach has not been tried. The challenge for this method is to make sure every

cell is visited. But in a sense this is much like the "super pixel" cell method used to solve (11) for DECam. The DECam cells are nearly the same size as ODI cells. On the other hand the plate scale is higher in ODI which would require even denser fields in good seeing conditions to achieve similar sampling.